

The Zeeman Effect of Lead II, III and IV

J. B. GREEN AND R. A. LORING, *Mendenhall Laboratory of Physics, Ohio State University*

(Received September 1, 1932)

Zeeman Effect of Pb II, III and IV, have been studied at fields of about 40,000 gauss with the newly completed outfit at the Mendenhall Laboratory. Gieseler's results on Pb II are in general correct, although a few minor discrepancies have been found. The $6d\ ^2D_3$ level shows an anomalous g -value which may be attributed to the fact that the $6d\ ^2D$ levels are inverted, or to perturbations

caused by neighboring configurations. In Pb III a similar perturbation is found in the $6s\ 7p$ configuration. Here the g -sum of 3P_1 and 1P_1 is slightly higher than the theoretical value, while the 3P_2 level, which should be unaffected by ordinary changes in coupling, yields a value 1.35 instead of 1.50.

CLASSIFICATIONS of the spark spectra of lead have been suggested by Gieseler¹ for Pb II and by Smith² for Pb III and Pb IV. Pb II shows a system of doublets and quartets and Pb III a system of singlets and triplets, while Pb IV shows doublets. The Zeeman effect for these spark spectra has not been measured except for a very few of the Pb II lines. Back³ has measured $\lambda 6660$, $\lambda 5608$ and $\lambda 2203$ and shown that they are $^2S-^2P$ transitions. Earlier work by Van der Harst⁴ indicated unresolved Zeeman patterns for $\lambda 5608$, $\lambda 4386$, $\lambda 4245$ and $\lambda 2698$. Kimura and Nakamura⁵ have classified the spectra into different degrees of ionization by means of the lengths of the lines in a condensed spark discharge. The present problem was undertaken to check the above classifications with the Zeeman effect patterns.

The apparatus consisted of a large Weiss type water-cooled electromagnet constructed in this laboratory, which gave a field strength of about 40,000 gauss when operated with a current of 90 amperes. Pole faces of 10 mm and about 3 mm pole gap were used. The magnet was operated well up on the saturated part of the magnetization curve, so that variations of 2-3 amperes in the current gave practically no variation in the

field strength. The spectroscopic apparatus consisted of a 21 foot concave grating ruled with 30,000 lines per inch by R. W. Wood, mounted in a Paschen-Runge mounting in the basement of this laboratory. Spectra from 2000A in the first order to 4000A in the third order could be observed simultaneously. The grating room, being well insulated, gave good temperature stability. To insure more constant temperature operating conditions, a wooden box, open on one side, was placed over the grating, and the temperature of the room itself was controlled by a thermostat. The extremely good definition of the Zeeman patterns, even with exposure times of 30 hours, showed that conditions were unusually good.

The light source was a rotating-disk vacuum arc similar to that used by the authors⁶ on the spectra of tin. It consisted of a thick walled brass vacuum chamber, placed so that the magnet pole pieces formed a part of the two sides, as shown in Fig. 1. Here HH' is the magnetic field axis. $BBBB$ shows the vacuum chamber; D is a brass disk 8 inches in diameter, which rotates counterclockwise in this figure about the axis A . This disk forms one electrode. The other electrode is a 1.5 mm brass or tungsten wire W , which slides vertically in a hollow brass rod C and touches D at the field axis. R is a hard rubber insulator, threaded to take the hollow brass tube G . Contact is made between W and G by a flexible wire F , which is fastened to the light brass weight E .

¹ Gieseler, *Zeits. f. Physik* **42**, 265 (1927).

² Smith, *Phys. Rev.* **34**, 393 (1929).

Smith, *Phys. Rev.* **36**, 1 (1930).

³ Back, *Zeits. f. Physik* **73**, 193 (1926).

⁴ Van der Harst, *Proc. Amster. Acad. Sci.* **22**, 300 (1920).

⁵ Kimura and Nakamura, *Japanese J. Phys.* **3**, No. 7-10, 197 (1924).

⁶ Green and Loring, *Phys. Rev.* **30**, 574 (1927).

A vacuum seal is maintained between *R* and *B* by soft wax and between *G* and *R* by a soft rubber gasket and stopcock grease. One electrical connection is made to the outside of *G*. Some slight adjustment of the centering of *W* may be obtained by sliding *R* on the top of the box. *K* is a long steel tapered shaft carrying a sprocket *L*

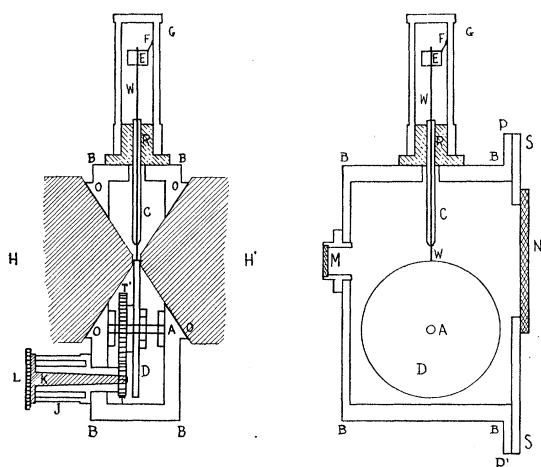


FIG. 1. Vacuum discharge source in magnetic field.

at one end and a small brass gear *T* at the other end, which in turn engages the gear, *T'*. This sprocket is connected by a chain drive to another sprocket and reducing gear. A motor drives the whole mechanism and causes the disk to rotate. Windows are placed in the front and back of the box at *M* and *N*. *M* is a fused quartz window cemented onto a brass collar which is fastened by soft wax to the vacuum box. *N* is a large plate glass window attached with soft wax to the back plate *S*. This plate covers the whole back of the vacuum box and can be removed for the purpose of changing the disk and cleaning the interior of the box. Soft wax seals are used here also as at *M* and *N*. Suitable manometer and pump connections make it possible to measure and maintain the vacuum.

The material used for the disk *D* depends upon the element being investigated. For the spectrum of zinc a $\frac{1}{8}$ inch brass disk and a 1.5 mm brass wire make a good combination. The principal *SP* multiplet lines are sufficiently strong to give a good exposure in about five minutes with an a.c. current of 3 amp., an air pressure of about 8 mm

of mercury, a $4\times$ normal slit-width in the spectroscopy and an Eastman 40 plate. For silver a 2 mm silver wire was silver soldered to the circumference of a copper disk and knurled flat. A tungsten wire made the other connection. For lead and tin a lead wire, a 40–60 solder wire or a tin wire was soldered on the rim of the wheel, knurled flat and used with a brass wire or a tungsten wire. For antimony and bismuth and other nonmalleable metals a brass disk may have its circumference turned down until it is about 1 mm thick and the metal cast on the outer surface and trued up in a lathe or in a grinding wheel.

The intensity of the discharge seems to depend somewhat upon the pressure between the wire and the disk and so it is necessary to experiment with the size of weight *E* and the stiffness of flexible wire *F*. The character of the arc is quite different when it takes place in the magnetic field. Without the presence of the field the arc strings out along the periphery of the disk. In the presence of the field and with the intersection of the disk and the wire exactly centered in the magnetic axis the spark appears to stretch out along the field and form a very narrow bright line. The character of the spectrum is decidedly different also. With no field the spectrum is arc-like in type, while, with a field, the first, second and third spark spectrum lines appear with good intensity and with no apparent diminishing of the arc lines. In the case of tin, some first, second and third spark lines that are very strong in the magnetic field are very weak lines or do not appear at all in a condensed spark. This is seen in the case of Sn $\lambda 5597$, Sn $\lambda 5369$ and Sn $\lambda 4215$.

In order to get the optimum operating conditions, a series of low-dispersion plates was made with a Gaertner constant deviation spectrograph. Five-minute exposures were made on d.c. Ortho plates with the pressure varying in steps of 1 mm from 4–20 mm of Hg, and a current of about 2 amp. and 110 volts a.c. An air pressure of 8 mm of Hg gave the most intense spark spectrum and the least intense band spectrum. Higher pressures made the arc more stable but the lines were not so sharp and the band spectrum became objectionable. A second series was run with hydrogen as residual gas.

A hydrogen atmosphere causes the discharge to become slightly more unstable although it is still manageable. The arc current was kept below 4 amp. to minimize spattering of small pieces of molten lead against the window. Even under these conditions it was necessary to clean the window every three hours to prevent excessive absorption of the light.

Twenty 2×10 inch Eastman 40 plates were set up in the blue and ultraviolet regions and, at the same time, four 2×10 inch W and W Panchromatic plates were set up in the first-order green and red regions. More recently we have found that the Eastman 1G Special Spectroscopic⁷ plates are much more satisfactory for the green region.

Altogether we made eleven exposures ranging from two hours to thirty hours net time. The first six sets were run without separating the polarizations. 40-60 solder was used on the rim of the disk. The last five exposures were run with lead strips cut from $\frac{1}{8}$ inch commercial lead sheeting soldered to the edge of the brass disk. Polarizations were separated by placing a large calcite crystal between the window *M* and the condensing lens of fused quartz of 12 inch focal length. Two 5X enlarged images were focussed at the slit about an inch apart horizontally, so that either polarization could be selected and introduced into the spectroscope with no chance of contamination by the other polarization. Even under the best operating conditions, it was necessary to change the wire *W* and clean the window *M* every three hours. The disk *D* had usually to be refaced after about fifteen hours.

The plates were developed in a modified Eastman D-76 fine-grain developer with 50 percent more than the recommended amount of sodium sulphite. They were fixed in an acid-hypo bath.

In the few years immediately following the proposal of Hund's theory of complex spectra, the Zeeman effect was used principally as a check on the classification of spectra but recent work on complex spectra has developed the necessity for accurate measurements of the magnetic splitting-factor *g*. With this idea in mind, the plates were dried slowly and carefully to prevent

possible distortions of the emulsion. They were then measured on a Société Gènevoise measuring engine. Each line was measured in five different positions along the length of the line, with two settings in each position. In several cases, the same line was remeasured on the same plate, and the agreement between the measured patterns for sharp lines was usually better than 0.5 percent.

With unresolved patterns, the method suggested by Shenstone and Blair⁸ were used for calculating *g*-values. One must, however, exercise considerable care and discretion in the application of these equations. It will be noted that the formulas apply only in case the blackening were proportional to the intensity of the light. Overexposure and plate inertia might serve to shift considerably the center of intensity of an unresolved group of lines. Thus, the relative intensities in a 5-line group vary theoretically from 1 to 15. With underexposure, the weaker lines may not appear at all because of plate inertia. The apparent center of intensity is thus shifted toward the stronger lines. With overexposure, the stronger lines are not blackened proportionately and the apparent center of intensity is shifted toward the weaker components. An example of this effect is shown by Table I.

TABLE I. *Effect of intensity on the apparent center of intensity of Pb 3176.**

Plate	Pattern	Order	Plate	Pattern	Order
My-6-d	(0) 1.151	I	My-1-7	(0) 1.111	II
My-6-6	(0) 1.111	II	My-1-16	(0) 1.099	III
My-6-16	(0) 1.089	III	A-19-6	(0) 1.158	II
My-1d	(0) 1.135	I			

* The theoretical pattern of this line consists of three groups of seven lines each. The intensity of the zero group is shaded with decreasing intensities symmetrically outward on both sides of the zero position. Its position, therefore, would be unaffected by change of intensity. The perpendicularly polarized components are each shaded outward with decreasing intensities. Note that the measured apparent center of intensity progresses inward with increasing diffraction order in the same set of plates (the intensity of the line decreases with increasing order number), and also that corresponding orders of different sets give consistent patterns, except A-19-6 which was about as strong in the second order as the other two sets in the first order.

⁷ Mees, J. Opt. Soc. Am. 21, 753 (1931).

⁸ Shenstone and Blair, Phil. Mag. 8, 765 (1929).

TABLE II. Zeeman effects in the first spark spectrum of Pb.

λ	ν	Classification (Gieseler ¹)	Pattern	Plates measured
2203	45367.7	$2^2P_2 - 2^2S_1$	(0.310) 0.99 1.68	3
2719	36756.8	$p^2D_2 - 5^2F_3$	(0) 1.07	1
2948	33903.1	$3^2D_3 - 5^2F_4$	(0) 0.95	2
3016	33140.1	$3^2D_2 - 5^2F_3$	(0) 0.84	3
3279	30480.4	$3^2P_2 - 5^2S_1$	(0) 0.91	4**
3452	28963.8	$p^2D_3 - 5^2F_4$	(0) 0.80	1
3718	26886.9	$3^2P_1 - 4^2S_1$	(.64) 1.30	3
3786	26404.0	$p^2D_2 - 4^2F_3$	(.40) (1.20) .44 1.08	5
3909	25574.4	$3^2D_2 - 4^2P_2$	(.30) 1.28	4
4153	24074.1	$3^2P_2 - 4^2S_1$	(.32) 1.01 1.60	2
4242	23566.2	$3^2D_3 - 4^2F_3$	(.18) (.65) (1.10) .20 .62 1.07 1.52 1.96	5
4245	23550.5	$3^2D_3 - 4^2F_4$	(0) 0.88	3
4386	22790.5	$3^2D_2 - 4^2F_3$	(0) 0.86	3
5042	19824.8	$p^4\bar{P}_1 - 3^2P_2$	(0) 0.84	2
5372	18609.5	$p^2D_3 - 4^2F_4$	(0) 0.47	2†
5608	17823.8	$2^2S_1 - 3^2P_2$	(.33) 1.00 1.67	2
5857	17067.6	$p^4\bar{P}_2 - 3^2P_2$	(0) 1.30	1*
5876	17012.4	$p^4\bar{P}_1 - 3^2P_1$	0.77	1

* Also assigned as Pb III $6^3D_3 - 7^3P_2$. (Smith².)

† Parallel components show six equally spaced lines with a separation of about 0.30.

** This classification is obviously incorrect. The pattern suggests an unresolved $2^2P_1^2D_2$ which calculates $\pm(1/15)$ 11/15 13/15.

Table II shows the measured Zeeman effects for the spectrum of Lead II, and Table III gives the g -values calculated from the patterns in Table II.

In addition to the remarks made in connection with the tables, we note the following interesting facts. The g -values for 3^2D_3 and 4^2F_3 calculated from the precision measurement on $\lambda 4242$ are 1.29 and 0.85 as compared with the theoretical values of 1.20 and 0.86. No theory has yet been proposed to account for perturbation of g -values of one-electron systems. We must therefore look for the explanation of the large perturbation in the g -value of 3^2D_3 in perturbations due to interactions of neighboring electronic configurations, or in the fact that the 3^2D terms are inverted. In the spectrum of Pb III we find similar difficulties which will be discussed later.

The quartet system also shows considerable perturbations, but here we have the case of a three-electron system (p^2s) and the g -values could be calculated by the method of Inglis and Johnston.⁹

The assignments given in Tables II and III are

⁹ Inglis and Johnston, Phys. Rev. **38**, 1642 (1931).

those of Gieseler,¹ and the authors' observations of the g -values indicate that the assignments are in general correct, although there is some room for doubt as to the validity of the classifications of the sp^2 configuration.

Table IV shows the measured Zeeman effects for Pb III, and Table V shows the g -values calculated from the measured patterns of Table IV.

The spectrum of Pb III offers an excellent opportunity for the comparison of theory and experiment. The theory of the Zeeman effect for two-electron systems of the simpler types has been developed by Houston¹⁰ and by Goudsmit,¹¹ along with the theory of multiplet separations. Discrepancies in the multiplet separations of 6^3D and 5^3F have already been noted by the authors.¹² The present work indicates serious discrepancies in the present status of the Zeeman effect according to this theory.

The $6s\ 7s^3S_1 - 6s\ 7p$ multiplet has been studied with especial care. This group of four lines appeared with very good intensity on all our plates, and were remarkably sharp for such high excita-

¹⁰ Houston, Phys. Rev. **33**, 297 (1929).

¹¹ Goudsmit, Phys. Rev. **35**, 1325 (1930).

¹² Green and Loring, Phys. Rev. **38**, 1289 (1931).

TABLE III. *g*-value table for Pb II.

	2^2P_2	$p^4\bar{P}_1$	2^2S_1	$p^4\bar{P}_2$	p^2D_2	p^2D_3	3^2P_1	3^2P_2	3^2D_2	3^2D_3	4^2S_1	4^2P_2	4^2F_3	4^2F_4	5^2F_3	5^2F_4
$\lambda 2203$	1.33		2.02													
2719					0.55										0.85	§
2948										1.29						1.14
3016									0.85						0.85	
3452						1.42										1.14
3718							0.66				1.94					†
3786					1.65								0.85			†
3909									1.16			1.40				†
4153								1.33			1.97					†
4242										1.29			0.85			†
4245									1.29					1.11		
4386									0.85				0.85			
5042		2.34						1.34								
5372						1.39								1.11		
5608			2.02					1.34								†
5857				1.27				1.33								
5876		2.20					0.66									
Mean	1.33	2.27	2.02	1.27	X	1.40	.66	1.33	.85	1.29	1.95	1.40	.85	1.11	.85	1.14
Theor.	1.33	2.67	2.00	1.73	.80	1.20	.67	1.33	.80	1.20	2.00	1.33	.86	1.14	.86	1.14

* This pattern is $\pm(0.30) 1.28$. The *g*-values chosen give $\pm(0.12) (0.36) 1.04 1.08 1.52$. If only the perpendicular components are matched we can take $g_1=0.85 g_2=1.71$. This line is assigned to the triplet system also. (Smith.² See Table IV.)
 † Precision measurement.
 ‡ This is an unusual type. It calculates with these *g*-values to give. $\pm(\overline{0.40}) (1.20) -\overline{0.35} 0.45 1.25 2.05$ which is good in comparison with the measured pattern of $\pm(\overline{0.40}) (1.20) 0.44 1.08$ Graphically the pattern is as shown in Fig. 2.

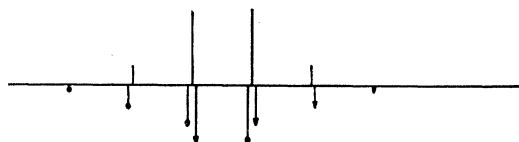


FIG. 2. Possible structure of Pb $\lambda 3786$.

§ This line may possibly be confused with a copper line. This line calculates at about $\lambda 2718.8$. The copper line is at $\lambda 2718.9$. Kayser lists a Pb line at $\lambda 2717.2$. A line appears on our plates at $\lambda 2717.5$. Gieseler, on the other hand, lists a Pb line at $\lambda 2719.78$. Our line at $\lambda 2717.5$ appears to have a pattern similar to that of $\lambda 3786$. It is not measurable due to its position on the plate.

tion spark lines. The intervals between the members of the $6s 7p$ levels are not in very good agreement with each other according to Houston's theory. However, if we calculate the parameters according to his suggestions, the *g*-values of 3P_1 and 1P_1 are in fairly good agreement with experiment. The *g*-sum which should be 2.50, is somewhat larger, 2.53, a value too high to be accounted for by experimental error. The *g*-value of the 3P_2 term which should be unaffected by changes in coupling turns out to be 1.34_8 ; instead of 1.50. There is no other level in the neighborhood whose combinations are sufficiently strong; so that the trouble cannot be attributed to incorrect classification. This suggests, then, a perturbation due to a level with $j=2$ from some

other configuration of electrons. An inspection of Table VIII (unclassified lines) suggests the possibility of such a level. The line $\lambda 4183$, from its Zeeman effect, appears to be a combination between a 3S_1 level and a level with $j=2$ and a *g*-value of 0.97. Strangely enough, the wave number of this line is exactly halfway between 7^3S_1 and 8^3S_1 , so that it might be either $7^3S_1 - x_2$ or $x_2 - 8^3S_1$, with $x_2 = 84,795$, and only 2034 wave numbers from 7^3P_2 , sufficiently close to produce a considerable perturbation.

In order for this level to produce a perturbation on the 3P_2 level, it is not sufficient that its *j*-value should be the same. Because of the nature of the integrals involved, Condon¹³ has shown that to

¹³ Condon, Phys. Rev. 36, 1121 (1930).

TABLE IV. Zeeman effects in the second spark spectrum of lead.

λ	ν	Classification (Smith ²)	Pattern	Plates measured
2562	39016.2	$6^1D_2-5^1F_3$	(0) 0.95	5
3031	32975.8	$6^3D_2-5^3F_3$	(0) 0.83	1
3044	32842.8	$6^3D_1-5^3F_2$	(0) 0.77	3
3089	32361.9	$6^3D_2-5^3F_2$	0.65 (1.02) 1.65	2
3138	31859.0	$6^3D_2-5^3F_3$	(0) 0.98	4
3176	31471.0	$6^3D_3-5^3F_4$	(0) 1.12	7
3242	30828.1	$6^3D_3-5^3F_3$	(0.64) 1.12	4
3276	30514.5	$7^3P_1-7^3D_2$	(0) 1.00	4
3280	30479.9	$7^3P_0-7^3D_1$	(0) 0.49	4
3297	30316.0	$7^3P_1-7^3D_1$	0.52 (0.86) 1.42	3
3689	27097.6	$6s\ 7s^3S_1-6s\ 7p^1P_1$	(0.849), 1.140, 1.972	7‡
3706	26974.7	$7^3P_0-8^3S_1$	(0) 2.00	3
3728	26810.5	$7^3P_1-8^3S_1$	(0.58) 1.32 2.00	4
3833	26083.0	$p^1D_2-5^3F_3$	(0) 0.51	4†
3841	26023.3	$7^3P_2-7^3D_3$	(0) 1.30	4
3854	25939.5	$7^3P_2-7^3S_1$	(0) (0.65) 0.68 1.33 1.97	6‡
3909	25573.7	$7^3P_2-7^3D_2$	(0.30) 1.27	4
3952	25296.9	$6s\ 6d^1D_2-6s\ 7p^1P_1$	(0) 1.01	3
4004	24967.0	$p^1D_2-5^3F_3$	(0) 0.78	1
4094	24415.1	$6s\ 7p^1P_1-6s\ 7d^3D_2$	(0) 1.15	1
4128	24316.8	$6s\ 7p^1P_1-6s\ 7d^3D_1$	0.54 1.06	1
4141	24139.5	$6^1D_2-7^3P_2$		1
4272	23398.2	$6s\ 7s^1S_0-6s\ 7p^1P_1$	(0) 1.14	4‡
4500	22218.4	$6s\ 7p^1P_1-6s\ 7d^1D_2$	(0) 1.13	2§
4571	21869.3	$7^3P_2-8^3S_1$	(0) (0.63) 0.65 1.29 1.91	3
4761	20998.0	$7^3P_1-7^3S_1$	(0.59) 1.38 1.98	6‡
4798	20834.0	$7^3P_0-7^3S_1$	(0) 1.98	5‡
5857	17067.5	$6^3D_3-7^3P_2$	(0) 1.30	1*

* Also assigned as Pb II $p^4\bar{P}_2-3^2P_2$
(Gieseler.¹ See Table II).
† Components broad—Shaded out.

‡ Precision measurement.
§ See text.
|| Only perpendicular components measurable.

TABLE V. g-values of Pb III.

Line	7^1S_0	7^3S_1	8^3S_1	7^3P_0	7^3P_1	7^3P_2	7^1P_1	6^1D_2	p^1D_2	6^3D_1	6^3D_2	6^3D_3	7^3D_1	7^3D_2	7^3D_3	7^1D_2	5^1F_3	5^3F_2	5^3F_3	5^3F_4	
2562								1.05										1.00			
3031											1.15							0.99			
3044										0.50								0.67			
3089											1.15							0.67			
3138											1.15									1.09	
3176												1.33									1.25
3242												1.33								1.09	
3276						1.38 ₃								1.13 ₃							
3280				√									0.49								
3297						1.38 ₂							0.52								
3689		1.97 ₆						1.14 ₉													
3706			2.00	√																	
3728			2.01			1.37 ₈															
3833										?										?	
3841								1.34 ₇								1.33 ₄					
3854		1.98 ₇						1.34 ₃													
3909								1.35 ₇								1.20 ₄					
3952								1.14 ₉	1.06												
4004										1.40										1.09	
4094								1.14 ₇							1.15 ₃						
4128								(1.06)						(0.54)							
4141						?			?												
4272	√							1.14 ₅													
4500								1.14 ₅								1.13 ₃					
4571			2.00					1.36 ₆													
4761			1.98 ₂					1.38 ₄													
4798			1.99 ₀	√																	
5857								1.34 ₅					1.32 ₅								
Aver.	√	1.98 ₃	2.00	√	1.38 ₃	1.34 ₃	1.14 ₇	1.06	1.40	0.50	1.15	1.33	0.50	1.16	1.33	1.14	1.00	0.67	1.09	1.25	
Theoretical	√	2.00	2.00	0/0	1.50	1.50	1.00	1.00	1.00	0.50	1.16 ₇	1.33 ₃	0.50	1.16 ₇	1.33 ₃	1.00	1.00	0.66 ₇	1.08 ₃	1.25	
Houston	√	2.00	2.00	√	1.37 ₁	1.50	1.12 ₉	1.00 ₁	?	0.50	1.16 ₆	1.33 ₃	0.50	1.16 ₆	1.33 ₃	1.00 ₁	?	0.66 ₇	?	1.25	

perturb each other both levels must belong to the same kind of electronic configuration, i.e., both of the configurations must be odd or both even. It would seem, therefore, that the level x_2 must belong to a pd configuration. In addition, it should be mentioned that the two levels need not necessarily be very close together to perturb each other. The perturbation calculation usually involves a term containing the difference in energy values of the perturbing terms in the denominator, and thus would ordinarily decrease as the distance between the terms increases. But if all the elements of the perturbation integral have the same phase for some interval, the value of the integral may be appreciable.

The accuracy of the measurements also indicates a discrepancy, just barely detectable, in the g -value of 7^3S_1 . The measured value is 1.98_3 , a value just on the limit of the accuracy of separable from the theoretical value 2. This effect does not come about as the result of the averaging of several discordant observations. Every line involving this level gives a g -value less than the theoretical.

Fig. 3 is included to show the effect on the Zeeman pattern of a change from ls to jj coupling. Fig. 3a is the Zn line $\lambda 4722$, II order, and 3b is the Pb III line $\lambda 4761$, I order. Both of these lines involve the same transition, $^3P_1 - ^3S_1$.

Fig. 4 shows the effect on the Zeeman pattern

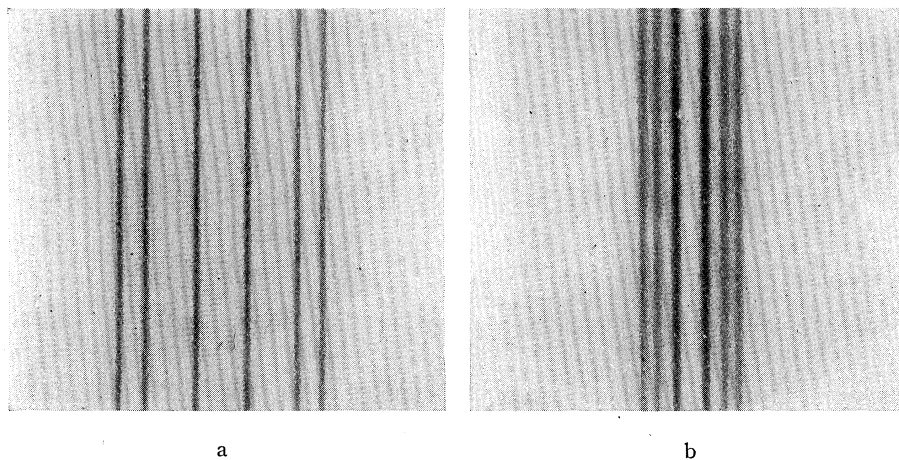


FIG. 3. (a) Zn 4722, II order, $L-S$ coupling. (b) Pb III 4761, I order, $J-J$ coupling.

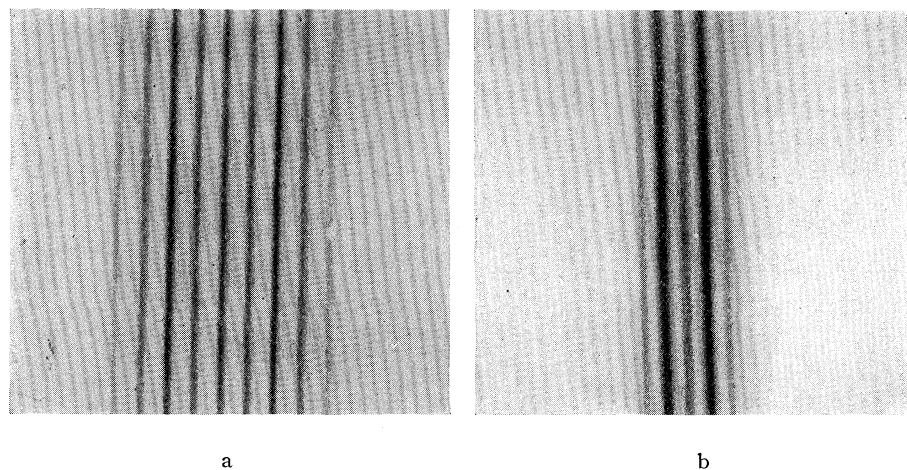


FIG. 4. (a) ZnI 4810, II order, LS coupling. (b) PbIII 3854, I order, JJ coupling.

of the perturbation of the g -value of the 3P_2 term. Fig. 4a is the Zn line $\lambda 4810$, II order, and 4b is the Pb III line, $\lambda 3854$; both lines involve the same transition, ${}^3P_2-{}^3S_1$. The blackest lines on the photograph Fig. 4b are overlapped parallel and perpendicular components, an effect which causes the pattern to look like a seven-line pattern instead of the nine-line pattern which it really is.

We should like also to suggest an alternate classification for the line $\lambda 4500$, classified by Smith as $6s\ 7p^1P_1-6s\ 7d^1D_2$. The level 1D_2 occurs in only one other transition, with $6s\ 6p^1P_1$,

TABLE VI. Zeeman effects in the third spark spectrum of lead.

λ	ν	Classification (Smith ²)	Pattern	Plates measured
2864	34899.4	$6d^2D_3-7p^2P_2$	0.21 (0.77) 1.76	5
3052	32748.8	$7s^2S_1-7p^2P_2$	(0.32) 0.97 1.62	4
3087	32383.5	$7p^2P_2-7d^2D_3$	(0) 1.11	1
3145	31781.3	$7p^2P_2-7d^2D_2$	—	1†
3221	31034.4	$6p^2D_3-7p^2P_2$	(0) 1.08	3
3962	25229.8	$6d^2D_2-7p^2P_1$	(0) 0.81	3*
4050	24685.7	$7s^2S_1-7p^2P_1$	(0.61) 1.28	3

* Smith² has suggested two alternative sets of classifications for Pb IV. This line is given the same classification in both sets.

† Not measurable, but qualitatively correct, i.e., the pattern shows that $\Delta j=0$.

TABLE VII. g -value table for Pb IV.

Line	$6d^2D_2$	$6d^2D_3$	$7s^2S_1$	$7p^2P_1$	$7p^2P_2$	$7d^2D_3$
2864						*
3052			1.939		1.295	
3087					1.295	
3221		1.174			1.295	1.19
3962	0.783			0.676		
4050			1.902			
Mean	0.783	1.174	1.92	0.676	1.295	1.19
Theor.	0.800	1.200	2.00	0.667	1.33	1.200

* The g -values for this pattern calculate to be $g_1=2.534$ and $g_2=0.986$ with $j_1=1/2$ and $j_2=3/2$. This was in an alternative classification which is obviously incorrect.

TABLE VIII. Magnetic resolution of unclassified lines in the lead spark.

λ	Pattern	Plates measured
2192	(0) 0.967	1
2242	(0) 1.17	1
2247	(0) 1.21 [-2.24]	1*
2568	(0) 0.917	1
2770	(0) 1.26	1
2977	(0) 1.63	1
2978	(0) 1.07	1
3455	(0) 1.17	3
3483	(0) 0.905	3
3586	(0) 1.02	3
3590	(0) 0.900	3
3593	(0) (0.89) 0 1.07	4
3655	(0) 0.92	3
3714	(0) 1.03	3
3736	(0) 1.13	3
3827	(0.58) 0.92	5
3993	(0) 0.94	1
4023	0.88	
4031	(0) 1.13	
4183	(0) (0.99) 0.95 1.91 [2.89]	†
4401	(0) 0.84 1.12	‡
4802	(0) 1.14	4
5545	(0) 1.07	2

* A fourth weak comp on short wave side at 2.24.

† Some doubt about 2.89 comp. Only appears on one side. See also text on Pb III.

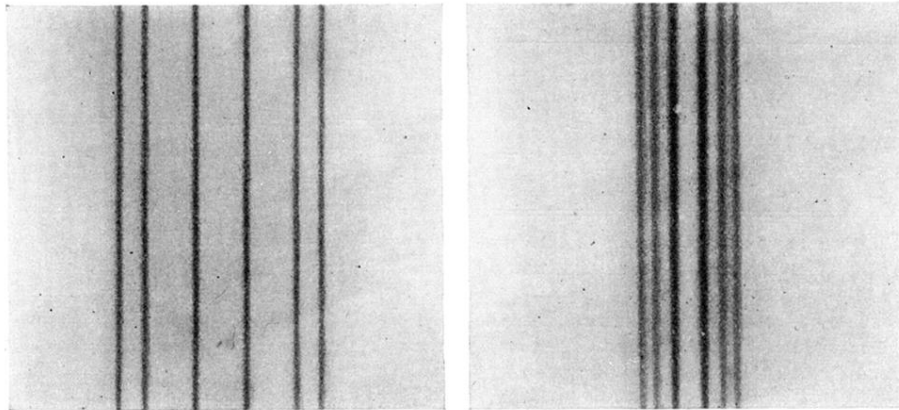
‡ Parallel component doubled on one plate; possible $\Delta j=0$.

and might, therefore, as well be 8^1S_0 , a classification much more consistent with the Zeeman pattern of 4500, and also consistent with the position of 8^3S_1 .

Table VI gives the measured Zeeman effects for the third spark spectrum of lead and Table VII gives the g -values calculated from these patterns.

The lines of Pb IV are not sufficiently sharp to be able to draw any conclusions from the g -factors the values of which fit the theoretical values within experimental error.

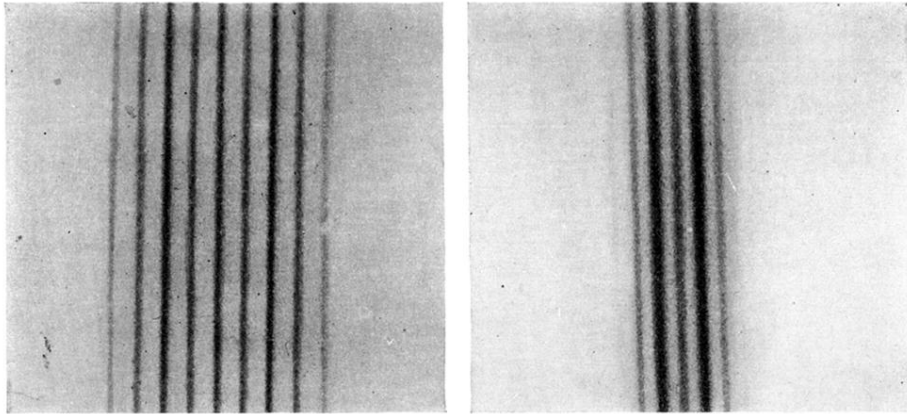
Table VIII shows the magnetic resolution of unclassified lines in the lead spark that appeared on our plates.



a

b

FIG. 3. (a) Zn 4722, II order, $L-S$ coupling. (b) Pb III 4761, I order, $J-J$ coupling.



a

b

FIG. 4. (a) ZnI 4810, II order, *LS* coupling. (b) PbIII 3854, I order, *JJ* coupling.